

Cite this article as: Zhang Junsong, Liao Jingjing, Wei Tianguo, et al. Oxygen Diffusion Behavior of Oxidized Zirconium Alloy During Vacuum Annealing Treatment[J]. Rare Metal Materials and Engineering, 2021, 50(05): 1590-1595.

ARTICLE

Oxygen Diffusion Behavior of Oxidized Zirconium Alloy During Vacuum Annealing Treatment

Zhang Junsong¹, Liao Jingjing^{1,2}, Wei Tianguo¹, Long Chongsheng¹

¹ Science and Technology on Reactor Fuel and Materials Laboratory, Nuclear Power Institute of China, Chengdu 610213, China; ² Department of Engineering Physics, Tsinghua University, Beijing 100084, China

Abstract: Vacuum heat treatments were performed at different temperatures for the Zr-Sn-Nb alloys which were already oxidized for a certain time. Results show that the oxide film dissolution into the matrix occurs during heat treatment, and the oxygen diffusion from zirconia to nearby zirconium matrix is enhanced. Diffusion kinetics of oxygen is discussed, and the diffusion coefficient is calculated for the specific alloy. The diffusion may be attributed to the existence of oxygen content gradient and the high oxygen solubility in the matrix. ZrO₂ is observed through microscopic chemical analysis, and the thickness of the metastable layer increases after the heat treatment. The thickness of oxygen-dissolved zirconium matrix (Zr(O)) layer also largely widens. It is speculated that in the actual aqueous corrosion procedure, there should be co-existence of oxidation and oxide film dissolution into the matrix. When the oxidation rate is restricted, the oxide film dissolution becomes obvious and facilitates the growth of metastable layer.

Key words: zirconium alloy; oxide film; vacuum annealing; diffusion kinetics; metastable phases

Zirconium alloys are the major structural materials used in pressurized-water reactor (PWR) due to their low thermal neutron absorption cross section, appropriate mechanical properties and good corrosion resistance. Corrosion of zirconium alloys has been the major consideration of many investigations. Especially with the requirements of high burn-up and extended operation time of reactor fuel, understanding corrosion behavior is of great challenges to researchers^[1].

Corrosion behavior of zirconium alloys has been widely investigated in the out-of-pile autoclave corrosion studies^[2]. Attention was paid on the micro-chemical and microstructures of the oxides generated on the alloy surface^[3,4]. Since monoclinic zirconia (m-ZrO₂) is the only stable phase of Zr-O binary compound at the corrosion temperature^[5], large areas of the oxides consist of the columnar m-ZrO₂. However, researchers have also observed a small content of metastable phases of Zr-O binary compounds at the oxide/metal interface^[6,7], such as tetragonal zirconia (t-ZrO₂), ZrO, Zr₂O, Zr₃O and etc^[8]. In some corroded alloys, the thin layer of suboxide was proved to locate at the metal/oxide interface^[9,10]. The existence of

metastable phases largely relates to the corrosion rate of alloys. Although sponge zirconium is not likely to form suboxide at the interface because of the quick corrosion rate, other finely designed alloys can commonly generate metastable phases at the interface due to much slower corrosion rate^[9,11]. A restricted corrosion rate facilitates the growth of metastable phases. The existence of metastable layer is very important to the corrosion resistance of alloys, but the formation mechanism is unclear.

It is suggested that the vacuum heat treatment experiment of oxidized zirconium alloys can help understand the diffusion kinetics of oxygen and the formation mechanism of metastable phase, since such treatment restricts the corrosion growth. Heretofore, most high temperature studies of Zr alloys were carried out in aqueous atmosphere which provides enough corrosion media to sustain the growth of oxide. Studies in the controlled atmosphere which restricts the growth of oxide are few. Oxide dissolution in such atmosphere has been proved by several researchers^[12,13]. However, structural and micro-chemical analysis of the deoxidized samples were not conducted.

Received date: May 09, 2020

Foundation item: National Natural Science Foundation of China (51771098)

Corresponding author: Long Chongsheng, Ph. D., Professor, Science and Technology on Reactor Fuel and Materials Laboratory, Nuclear Power Institute of China, Chengdu 610213, P. R. China, Tel: 0086-28-85903014, E-mail: ewiges@126.com

Copyright © 2021, Northwest Institute for Nonferrous Metal Research. Published by Science Press. All rights reserved.

This study aims to further analyze the oxide film dissolution into the matrix of oxidized zirconium alloy. The micro-structure and micro-chemical analysis of deoxidized samples were investigated to explore the diffusion kinetics of oxygen and formation mechanism of metastable phases.

1 Experiment

Zr-Sn-Nb alloy with the nominal composition of Zr-1Sn-0.3Nb-0.3Fe was provided by Nuclear Power Institute of China (NPIC). In this research, Zr-Sn-Nb alloy was corroded under the condition of 360 °C/18.6 MPa in the pure water to obtain the oxide film with thickness of about 1 μm . Several samples were put into stainless steel tubes with 40 mm in diameter and 80 mm in length. The tubes were filled with sponge zirconium to prevent the residual oxygen in the tube. Then the tubes were evacuated, sealed and finally annealed at different temperatures in a tubular vacuum furnace at a pressure of 10^{-4} Pa. Afterwards, the specimens were slowly cooled down to room temperature. The mass of treated samples was recorded before and after heat treatments.

The samples were cut and mounted in the hot mounting resin. In order to obtain a smooth face of the cross section of oxide film, firstly the samples were mechanically polished and then vibro-polished at the cross section by colloidal alumina for 6 h. The oxide films were well preserved during sample preparation when the samples were mounted closely to each other.

Morphologies of the cross section were achieved by FEI Nova 400 scanning electronic microscopy (SEM) in backscattered mode. The energy-dispersed spectrum (EDS) equipped on SEM was mainly used to analyze the surface micro-chemical conditions. Grazing incidence X-ray diffraction (XRD) can be used to analyze phase structure of the oxide films. Grazing incidence angle of 1° was chosen for XRD characterization and the corresponding X-ray probing thickness was estimated as 0.5 μm ^[14].

As a qualitative analysis method, EDS can provide the oxygen atomic content of the oxidized samples, but the space resolution should be considered as well. Many EDS scanning studies on the SEM provided spectra of rapid oxygen gradient

from zirconia phase to zirconium phase at the metal/oxide interface^[11]. Even though there was suboxide layer with tens of nanometers in thickness, the information was covered because of relatively poor resolution of the EDS on SEM. A space resolution of 100 nm was expected for EDS equipped on field emission SEM (FESEM). Therefore, only thick suboxide layer can be identified by the EDS on FESEM. Since the suboxide and oxygen-dissolved layers were thick after anneal treatment, the application of EDS on FESEM was credible.

2 Results

2.1 Structures of oxidized samples after vacuum heat treatment

Fig.1 is the SEM images of the samples annealed at different temperatures for 6 h. It can be seen that the thickness of the oxide film is about 1 μm before annealing treatment and there is an oxygen containing substrate region (known as α -case) of hundreds of nanometers in thickness beneath the metal/oxide interface. This α -case region can be observed and the morphology difference between this region and nearby substrate region is quite obvious. This region is marked as α -case, as shown by the dash line in Fig. 1a~1c. Because the equiaxed grains of α -Zr are the major structure in this layer, it is suggested that the α -Zr structure is stabilized by a relatively high oxygen content, which can be used to evaluate the diffusion procedure of different heat treatments^[12].

After anneal at 600 °C, the oxygen in the oxide film diffuses to the substrate continuously, and the thickness of oxide film decreases to 500 nm. The α -case area gradually widens to 3.4 μm . After anneal at 700 °C, the oxide film almost dissolves and the α -case area widens to about 6 μm . After the sample is annealed at 800 °C, the oxygen diffuses completely into the zirconium matrix and no obvious structure differences are observed.

The results demonstrate that oxide film gradually dissolves at high temperature. The mass of samples before and after anneal does not change, which indicates that the oxygen dissolves into the metal matrix and is not released to the vacuum atmosphere.

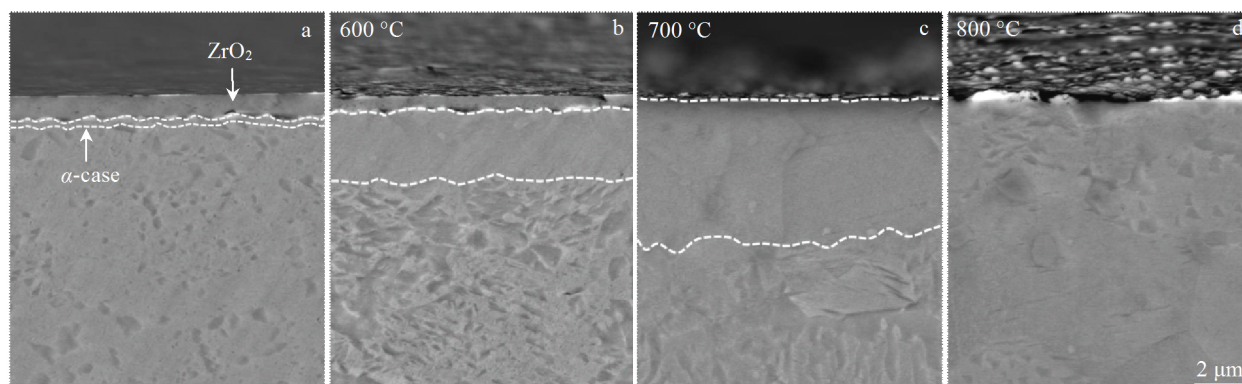


Fig.1 SEM images of zirconium alloys before (a) (as-recieved) and after anneal in vacuum at different temperatures for 6 h: (b) 600 °C, (c) 700 °C, and (d) 800 °C

Fig.2 shows the XRD patterns of the dissolved films forming on samples with different treatments. There are diffraction peaks of monoclinic phase $m(\bar{1}11)$ in the sample annealed at 600 °C for 6 h in vacuum, which is consistent with untreated sample. All the patterns exhibit the characteristic peaks of zirconium matrix $Zr(002)$ and $Zr(101)$. These peaks are almost in good agreement with α -Zr, but the difference is that the 2θ values of all the samples are slightly smaller than those of α -Zr for every peak. According to the diffraction principle, the distance of corresponding crystal plane can be calculated as follows:

$$\lambda = 2d \sin \theta \tag{1}$$

where λ is the wavelength of X-ray, d is the interplanar spacing and θ is the diffraction angle. The interplanar spacing value of each treated sample relates to the oxygen contents at the interfacial region determined by EDS.

From low dissolved oxygen content to high dissolved oxygen content, the θ value decreases and d value increases. The

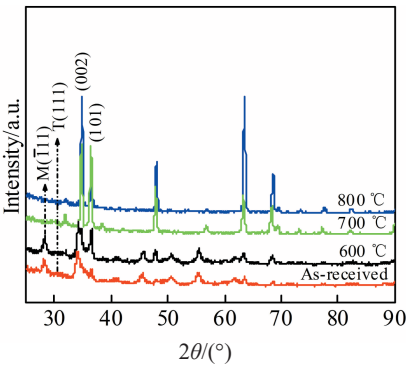


Fig.2 XRD patterns of oxide film of zirconium alloys before and after anneal at different temperatures

result indicates that the crystal lattice is expanded after oxygen dissolution. With higher content, the increase of lattice parameter becomes more obvious. After the oxygen from zirconia diffuses into the zirconium matrix via vacuum heat treatment, the oxygen mostly dissolves into the nearby matrix with content no more than the upper dissolution limit (~29at% at room temperature). As oxygen mainly exists at the interstitial sites of the lattice, the oxygen dissolution thereby expands the interplanar spacing. Higher content of oxygen dissolution increases the distortion of matrix lattice and exhibits larger lattice displacement, resulting in the experiment phenomenon.

2.2 Oxygen diffusion of annealed samples

2.2.1 Micro-chemical analysis of oxygen

EDS was used to qualitatively measure the oxygen diffusion in the surface layers. Fig.3 shows the SEM images and EDS results of untreated sample and samples annealed at 600, 700 and 800 °C for 6 h. Originally, the oxide keeps in good stoichiometry of ZrO_2 phase. The oxygen content decreases rapidly from 66at% to 20at%, which shows no obvious existence of metastable Zr-O phases. At the initial corrosion stage, the oxide is still relatively loose and the formation of metastable phase and saturated oxygen layer is not likely to be observed in the oxidized samples with thin film. As shown in Fig. 3b, the thickness of oxide film decreases from 1 μm to 500 nm after anneal at 600 °C for 6 h. In the oxide film, the content of Zr and O is consistent with the zirconia phase. However, in this sample, the content of oxygen decreases slower at the metal/oxide interface than that in the as-received sample does. There is a layer of about 300 nm in thickness with the oxygen content of 48at%~55at%. Many investigations demonstrate the existence of suboxides with the oxygen content of 50at% and other metastable phases in form of Zr_2O and Zr_3O at the interface^[6,7,9]. Since the upper limit dissolution of oxygen in matrix is about 29at%, the observed layer cannot

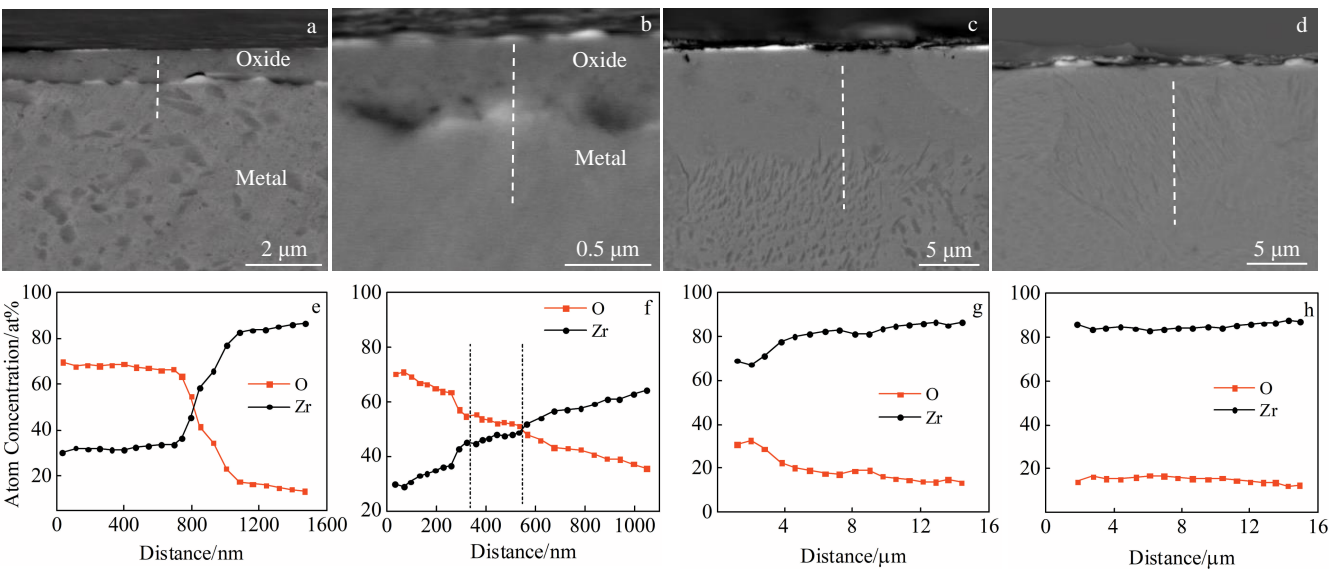


Fig.3 SEM images (a~d) and EDS results (e~h) of samples before (a, e) and after anneal at 600 °C (b, f), 700 °C (c, g), and 800 °C (d, h) for 6 h

be considered as the dissolved oxygen in matrix or zirconia, but a layer of metastable phases. ZrO is the dominant phase. Beneath the suboxide layer, the oxygen decreases gradually along the direction of matrix, providing a continuous oxygen gradient which promotes the zirconia dissolution.

The oxide film disappears in samples annealed at 700 and 800 °C for 6 h. But the diffusion degree of oxygen of two samples is not the same. The oxygen content is about 29at% in the outermost matrix and there is still an obvious oxygen content gradient in the sample annealed at 700 °C for 6 h. It takes about 15 μm in length for the oxygen content decreasing from 29at% to 10at%. The oxygen content of the sample annealed at 800 °C for 6 h is about 19at% at the outermost side and the oxygen gradient is much smaller, which indicates the adequate oxygen diffusion. In the two samples, the main form of oxygen is interstitial atoms in the lattice. Since the oxygen content does not exceed the upper dissolution limit, there is no metastable phase.

2.2.2 Diffusion kinetics of oxygen atoms in zirconium matrix

Diffusion coefficient D is the basic physical parameter to characterize the diffusion speed. It can be calculated by Fick's second law, as indicated in Eq.(2) as follows:

$$\frac{\partial c}{\partial t} = D \frac{\partial^2 c}{\partial x^2} \quad (2)$$

where c is the concentration of element, t is the time and x is the diffusion length. The differential equation can be solved with an error function (erf) with the boundary conditions of $c_1(x=0)=30\text{at\%}$ and $c_0(x \rightarrow \infty)=0\text{at\%}$, as indicated in Eq.(3) as follows:

$$c(x, t) = c_1 - (c_1 - c_0) \operatorname{erf}\left(\frac{x}{2\sqrt{Dt}}\right) \quad (3)$$

Two more samples were annealed at 500 °C for 35 h and

400 °C for 200 h separately for diffusion kinetics studies and the results of oxygen content are shown in Fig.4. The oxide films of both samples slightly dissolve. At 500 °C, the oxygen content drops smoother than that of the as-received sample does. Even though there is no obvious content gradient of ZrO layer, the thicker layer between zirconia and oxygen-dissolved matrix suggests the existence of metastable phases. At even lower anneal temperature, the diffusion is much slower and it takes longer time for the oxide to dissolve. The anneal treatment enlarges the oxygen-dissolved region beneath the metal/oxide interface.

According to Fig.3f and Fig.4, the diffusion coefficient of oxygen in zirconium matrix at corresponding temperature can be calculated, as shown in Table 1.

The diffusion coefficient D is temperature dependent according to Arrhenius relationship (Eq.(4)) and can be used to calculate the activation energy Q for oxygen diffusion in the zirconium lattice.

$$D = D_0 e^{-\frac{Q}{RT}} \quad (4)$$

where D_0 represents the diffusion prefactor, R is the gas constant, and T is the temperature. A linear fit of the data leads to result of activation energy $Q_{Zr}=143 \text{ kJ/mol}$ (Fig.5). Therefore, Eq.(4) can be used to calculate the diffusion coefficient D at different temperatures.

3 Discussions

3.1 Oxygen diffusion mechanism during oxide film dissolution

During the corrosion process, as shown in Fig.6, the electric potential is established between the oxide/metal interface and oxide/water interface. This potential is able to drive the

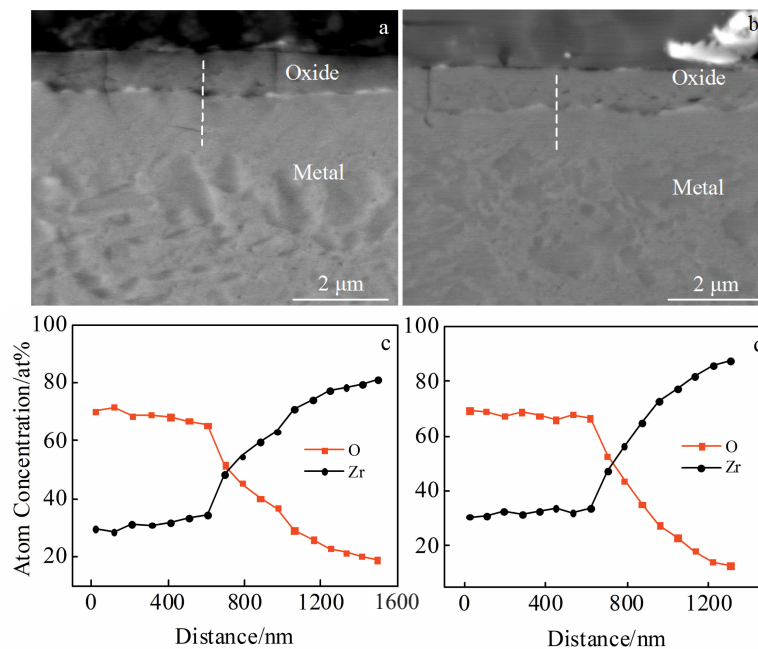


Fig.4 SEM images (a, b) and EDS results (c, d) of samples annealed at 500 °C for 35 h (a, c) and 400 °C for 200 h (b, d)

Table 1 Diffusion length, oxygen concentration, and diffusion coefficient of oxygen in zirconium matrix at different temperatures

Anneal treatment	Diffusion length, x/m	Oxygen concentration, $c/\text{at}\%$	Diffusion coefficient, $D/\text{m}^2\cdot\text{s}^{-1}$
600 °C/6 h	1.69×10^{-6}	18.83	2.86×10^{-16}
500 °C/35 h	8.06×10^{-7}	19.85	1.34×10^{-17}
400 °C/200 h	5.13×10^{-7}	19.24	0.80×10^{-18}

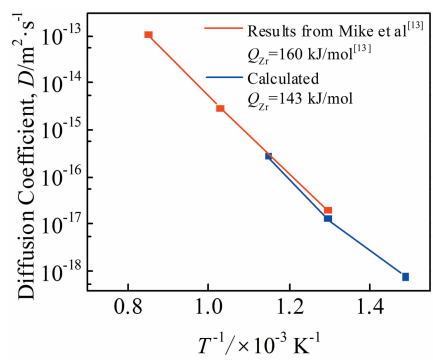


Fig.5 Activation energy for oxygen diffusion trough the zirconium lattice

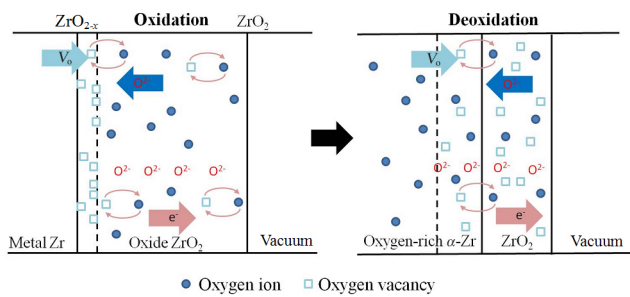


Fig.6 Schematic diagram of diffusion in zirconium alloy oxide film during oxidation and oxide film dissolution

charged species to migrate across the oxide film. The electric potential driving force is one order of magnitude higher than the concentration gradient driving force, and the electric field lowers the migration energy barrier for vacancy diffusion process^[15]. Consequently, the oxygen vacancies migrate to the oxide/water interface via these driving forces at high temperature.

When the corroded samples are annealed in vacuum, there is little external oxygen dissociated at the oxide/vacuum interface. The growth of oxide film is restricted and the dissolution process of oxide film on the corroded samples is much more obvious. Since zirconium matrix is able to dissolve oxygen with a very high content, the oxygen from the interfacial zirconia phase is likely to move into the nearby zirconium lattice at high temperature. Oxygen atoms in the oxide film continuous-

ly dissolve into the metal substrate with the help of oxygen gradient in different layers, which thins the original oxide film. As a result, the oxide/vacuum interface remains, and the oxide/metal interface constantly moves to the outer side of the oxide film. A thick layer of oxygen-dissolved zirconium then forms. The length of the diffusion path for oxygen extends and oxygen content gradually decreases. During this procedure, the metastable phases are generated at the metal/oxide interface because of complex chemical sub-stoichiometry.

It is found that even at relatively low temperature (about 400 °C), the oxygen diffusion from the interfacial zirconia into the metal matrix still exists, which suggests that during the aqueous corrosion, the oxide film dissolution procedure also occurs. Under the aqueous corrosion condition, the oxidation and oxide film dissolution procedures exist at the same time. Since the corrosion media is adequate for oxide growth, oxidation is the dominant procedure. Since the oxide of finely designed alloys can become very dense and the oxidation rate is largely restricted in a long period of time^[3,4], oxide film dissolution procedure becomes active and shows obvious effects at the interface.

3.2 Formation of metastable phases at interface

In the vacuum atmosphere, the formation of metastable phases is confirmed by EDS results. As oxide growth stops, the continuous dissolution of oxygen atoms generates thicker oxygen-dissolved layer. When oxygen dissolves to the upper solution limit of zirconium matrix, an oxygen-saturated layer ($\text{Zr}(\text{O})_{\text{sat}}$) forms^[7]. Since the oxygen atoms continuously move into the oxygen-saturated layer because of existing oxygen gradient between ZrO_2 and $\text{Zr}(\text{O})_{\text{sat}}$, it is much likely to induce the formation of suboxide or other metastable phases to release the free energy. Therefore, it is expected that the restricted corrosion rate facilitates the growth of metastable phases.

Some researches indicated the similar relationship between the low corrosion rate and the existence of metastable phases. Studies showed the existence of thicker suboxide in the passivated alloys with low corrosion rate^[6] and at the interfacial positions with low local corrosion rate^[8,11]. In both cases, the oxidation rate is restricted, which promotes the oxide film dissolution into the matrix during oxidation procedure. From this point of view, formation of metastable phases is the result of good corrosion resistance. It is observed that the thickness of t- ZrO_2 layer gradually increases in the pre-transition stage^[16], which can be also proposed as the result of restricted corrosion rate.

4 Conclusions

1) Zirconium has high oxygen solubility (~29at% at room temperature in α -Zr) and can dissolve its own oxide film during the vacuum heat treatment. The oxide thickness decreases, and the oxygen diffusion from zirconia to the matrix is enhanced.

2) The oxygen rich α -Zr and metastable layers thicken during the oxide film dissolution procedure. It is proposed that the oxygen gradient in different layers have a major impact on

diffusion kinetics.

3) The restricted corrosion rate during the heat treatment is likely to facilitate the growth of metastable phases. In the aqueous corrosion situation, the oxidation and oxide film dissolution both exist. When the oxidation rate is restricted because of the dense oxide structure, the oxide film dissolution into matrix exhibits obvious effects on the interfacial metastable layer.

References

- Motta A T, Couet A, Comstock R J. *Annual Review of Materials Research*[J], 2015, 45: 311
- Liao J J, Yang Z B, Qiu S Y et al. *Acta Metallurgica Sinica, English Letters*[J], 2019, 32(8): 981
- Preuss M, Frankel P, Lozano-Perez S et al. *Journal of ASTM International*[J], 2011, 8(9): 1
- Yilmazbayhan A, Motta A T, Comstock R J et al. *Journal of Nuclear Materials*[J], 2004, 324(1): 6
- Aryanfar A, Thomas J, Ven A V D et al. *Journal of Materials*[J], 2016, 68(11): 2900
- Hu J, Garner A, Ni N et al. *Micron*[J], 2015, 69: 35
- Ni N, Hudson D, Wei J et al. *Acta Materialia*[J], 2012, 60(20): 7132
- Liao J J, Xu F, Peng Q et al. *Journal of Nuclear Materials*[J], 2020, 528: 151 846
- Yan D. *Thesis for Doctorate*[D]. Detroit: University of Michigan, 2017
- Kurpaska L, Jozwik I, Jagielski J. *Journal of Nuclear Materials* [J], 2016, 476: 56
- Liao J J, Yang Z B, Qiu S Y et al. *Journal of Nuclear Materials* [J], 2019, 524: 101
- Pawar V, Weaver C, Jani S. *Applied Surface Science*[J], 2011, 257(14): 6118
- Mosbacher M, Scherm F, Glatzel U. *Surface & Coatings Technology*[J], 2018, 339: 139
- Gosset D, Le Saux M, Simeone D et al. *Journal of Nuclear Materials*[J], 2012, 429(1-3): 19
- Couet A, Motta A T, Ambard A. *Corrosion Science*[J], 2015, 100: 73
- Wei J, Frankel P, Polatidis E et al. *Acta Materialia*[J], 2013, 61 (11): 4200

锆合金氧化膜在真空退火过程中的氧扩散行为

张君松¹, 廖京京^{1,2}, 韦天国¹, 龙冲生¹

(1. 中国核动力研究设计院 反应堆燃料及材料重点实验室, 四川 成都 610213)

(2. 清华大学 工程物理系, 北京 100084)

摘 要: 针对已预腐蚀生成一定厚度氧化膜的Zr-Sn-Nb合金, 研究了其在不同温度下进行真空热处理过程中的氧扩散动力学及亚稳相演变行为。结果表明, 真空退火后氧化膜变薄, 氧在氧化锆基体中的扩散增强, 并计算了特定合金中氧的扩散系数。退火后微观化学分析表明亚稳相层厚度增加。固溶氧锆基体(Zr(O))层也明显增厚。针对该现象, 讨论了对应氧扩散及亚稳相形成过程: 该扩散极为可能是由ZrO₂和Zr(O)之间存在的氧含量梯度以及锆基体的高氧溶解度造成, 受抑制的氧化速率将促进亚稳相的生长。在实际水腐蚀情况下, 氧化及氧化膜向基体溶解过程应该是共存的。当氧化速率受限时, 氧化膜向基体溶解作用将增强, 有利于形成较厚的亚稳层。

关键词: 锆合金; 氧化膜; 真空退火; 扩散动力学; 亚氧化相

作者简介: 张君松, 女, 1988年生, 博士生, 中国核动力研究设计院反应堆燃料及材料重点实验室, 四川 成都 610213, 电话: 028-85903377, E-mail: 659979076@qq.com